MGL1 promotes adipose tissue inflammation and insulin resistance by regulating 7/4^{hi} monocytes in obesity

Daniel J. Westcott,[1,3] Jennifer B. DelProposto,[1] Lynn M. Geletka,[1] Tianyi Wang,[1] Kanakadurga Singer,[1] Alan R. Saltiel,[4,2] and Carey N. Lumeng[1,2]

[1]Department of Pediatrics and Communicable Diseases, [2]Molecular and Integrative Physiology, University of Michigan Medical School, [3]Literature, Sciences and Arts Program, [4]Life Sciences Institute, University of Michigan, Ann Arbor, MI 48109

Adipose tissue macrophages (ATMs) play a critical role in obesity-induced inflammation and insulin resistance. Distinct subtypes of ATMs have been identified that differentially express macrophage galactose-type C-type lectin 1 (MGL1/CD301), a marker of alternatively activated macrophages. To evaluate if MGL1 is required for the anti-inflammatory function of resident (type 2) MGL1$^+$ ATMs, we examined the effects of diet-induced obesity (DIO) on inflammation and metabolism in *Mgl1*$^{-/-}$ mice. We found that *Mgl1* is not required for the trafficking of type 2 ATMs to adipose tissue. Surprisingly, obese *Mgl1*$^{-/-}$ mice were protected from glucose intolerance, insulin resistance, and steatosis despite having more visceral fat. This protection was caused by a significant decrease in inflammatory (type 1) CD11c$^+$ ATMs in the visceral adipose tissue of *Mgl1*$^{-/-}$ mice. MGL1 was expressed specifically in 7/4^{hi} inflammatory monocytes in the blood and obese *Mgl1*$^{-/-}$ mice had lower levels of 7/4^{hi} monocytes. *Mgl1*$^{-/-}$ monocytes had decreased half-life after adoptive transfer and demonstrated decreased adhesion to adipocytes indicating a role for MGL1 in the regulation of monocyte function. This study identifies MGL1 as a novel regulator of inflammatory monocyte trafficking to adipose tissue in response to DIO.

CORRESPONDENCE
Carey Lumeng:
clumeng@umich.edu

Abbreviations used: ATM, adipose tissue macrophages; CLS, crownlike structure; DIO, diet-induced obesity; EWAT, epididymal white adipose tissue; FFA, serum-free fatty acid; HFD, high-fat diet; MGL, macrophage galactose-type C-type lectin; ND, normal diet; PM, peritoneal macrophage; SVF, stromal vascular fraction; TG, thioglycollate .

Chronic inflammation is an important consequence of obesity that impacts upon the development of insulin resistance, diabetes, and metabolic syndrome (Hotamisligil, 2006; Neels and Olefsky, 2006). Obesity-induced systemic inflammation is characterized by chronic elevations in circulating inflammatory cytokines (e.g., TNF and IL-6), adipokines, and monocytes (Hotamisligil et al., 1995; Ghanim et al., 2004). At the tissue level, inflammatory pathways are induced in visceral adipose tissue that lead to a striking accumulation of macrophages (Weisberg et al., 2003; Xu et al., 2003). These adipose tissue macrophages (ATMs) are now recognized to be a significant participant in the inflammatory response to obesity as they generate a wide range of inflammatory cytokines in hypertrophied adipose tissue (Coppack, 2001). Attenuation of inflammatory genes such as *Jnk1* and *Ikkb* in macrophages has been shown to decrease inflammation and prevent the development of insulin resistance and glucose intolerance with diet-induced obesity (DIO; Arkan et al., 2005; Solinas et al., 2007). Signals between inflammatory ATMs and adipocytes impair insulin sensitivity in adipocytes and influence adipocyte cell death (Cinti et al., 2005; Lumeng et al., 2007a).

The biology of ATMs in both lean and obese states is slowly being revealed. ATMs are derived from the bone marrow and differentiate in adipose tissue from circulating monocytes (Weisberg et al., 2003). Two distinct types of ATMs have been identified. ATMs in obese mice have an activation pattern similar to that seen with classical or M1 macrophage activation, with high expression of *Tnfa*, *Il6*, and *Nos2* (Lumeng et al., 2007b). We will refer to these cells as type 1 ATMs and define them as F4/80$^+$ CD11c$^+$ macrophage galactose-type C-type lectin$^-$ 1 (MGL1$^-$; Lumeng et al., 2007b, 2008;

D.J. Westcott and J.B. DelProposto contributed equally to this paper.

The Rockefeller University Press $30.00
J. Exp. Med. Vol. 206 No. 13 3143-3156
www.jem.org/cgi/doi/10.1084/jem.20091333

Nguyen et al., 2007). Type 1 ATMs organize themselves into clusters that have been described as "crownlike structures" (CLSs) that are closely coupled to adipocyte death (Cinti et al., 2005; Murano et al., 2008). These ATMs ingest triglyceride and take on an appearance similar to foam cells (Cinti et al., 2005; Lumeng et al., 2007a).

A second population of ATMs has the phenotype F4/80$^+$ CD11c$^-$ MGL1$^+$; we will refer to these as type 2 ATMs (Lumeng et al., 2008). These ATMs are the predominant macrophage type in adipose tissue in lean mice and express genes that overlap with alternatively activated or M2 macrophages, such as *Arg1*, *Il10*, *Mgl1*, and *Mgl2* (Lumeng et al., 2007b). Type 2 ATMs localize in interstitial spaces between adipocytes and are present in both lean and obese states. It is believed that the alternative activation state of type 2 ATMs maintains homeostasis by suppressing proinflammatory signals activated with obesity as macrophage-specific knockouts of *Pparg* and *Ppard* demonstrate worse insulin resistance and inflammation (Hevener et al., 2007; Odegaard et al., 2007; Kang et al., 2008).

Type 2 ATMs predominate in lean mice, whereas obesity induces the accumulation of type 1 ATMs leading to a proinflammatory environment (Lumeng et al., 2007b). The mechanism behind this shift in ATM phenotype may relate to the differential recruitment of monocyte subtypes to adipose tissue (Weisberg et al., 2006; Gordon, 2007; Lumeng et al., 2008; Nishimura et al., 2008). In mice, a population of 7/4^{hi} CCR2$^+$ Ly-6C^{hi} CX_3CR1^{lo} monocytes are preferentially recruited to sites of tissue inflammation and generate classically activated macrophages (Gordon and Taylor, 2005; Gordon, 2007). In contrast, 7/4^{mid} CCR2$^-$ Ly-6C^{lo} CX_3CR1^{hi} monocytes appear to be regulated by different stimuli and may play a role in patrolling noninflamed tissues that give rise to resident tissue macrophages (Geissmann et al., 2003; Auffray et al., 2007; Bouhlel et al., 2007; Charo, 2007). Importantly, 7/4^{hi} monocytes are increased with obesity, suggesting that they may be a specific inflammatory mediator of obesity-induced inflammation (Tsou et al., 2007).

Type 2 ATMs express high levels of macrophage galactose-type C lectin 1 (MGL1/CD301), a marker of alternatively activated macrophages (Kang et al., 2008; van Kooyk, 2008). MGL1 is type 2 transmembrane protein expressed on macrophages and DCs in multiple tissues that is part of a family of scavenger receptors including macrophage mannose receptor (CD206; van Kooyk, 2008; van Vliet et al., 2008a). Functions for mMGL1, its homologue mMGL2, and human MGL in DCs include antigen presentation, suppression of effector T cell function, and negative regulation of cell migration (van Vliet et al., 2006, 2008a, 2008b). mMGL1 has binding specificity for Lewis X and Lewis A structures, which differentiates it from mMGL2 and hMGL (Tsuiji et al., 2002; Singh et al., 2009). MGL1 ligands include sialoadhesin, apoptotic cells, and commensal bacteria such as *Streptococcus sp.* (Kumamoto et al., 2004; Yuita et al., 2005; Saba et al., 2009). This latter interaction triggers production of IL-10 in macrophages and explains the increased inflammation seen with experimental colitis in *Mgl1*$^{-/-}$ mice (Saba et al., 2009).

We sought to examine the role of MGL1 in obesity-induced inflammation and insulin resistance by evaluating the response of *Mgl1*$^{-/-}$ mice to DIO. We hypothesized that the protective functions of type 2 ATMs would be attenuated in *Mgl1*$^{-/-}$ mice, and that they would show increased inflammation and worse insulin resistance. Surprisingly, we observed the opposite result as obese *Mgl1*$^{-/-}$ mice had improved glucose tolerance and impaired accumulation of type 1 ATMs in visceral adipose tissue. The mechanism of this effect is related to the expression of MGL1 on inflammatory 7/4^{hi} monocytes and the lack of maintenance of these monocytes in the circulation caused by the intrinsic properties of *Mgl1*$^{-/-}$ monocytes. Overall, we demonstrate that MGL1 is a novel cell surface receptor involved in the regulation of monocyte/macrophage activation and trafficking to fat in obesity.

RESULTS

Type 2 ATMs do not require MGL1 to traffic properly to adipose tissue

We have previously shown that the resident population of type 2 ATMs expresses high levels of MGL1 (Lumeng et al., 2008). We hypothesized that MGL1 might participate in the recruitment of these ATMs to fat. To test this, we examined ATMs from *Mgl1*$^{-/-}$ mice fed a normal chow diet (ND) by immunofluorescence. ATMs were present in *Mgl1*$^{-/-}$ mice with a morphology and density that was identical to WT controls (Fig. 1 A). ATMs in *Mgl1*$^{-/-}$ and WT mice expressed CX_3CR1 and the M2 macrophage marker, CD206/mannose receptor. Quantitation of ATMs in epididymal fat pads from ND mice by flow cytometry showed no difference in the quantity of F4/80$^+$ CD206$^+$ ATMs between *Mgl1*$^{-/-}$ mice and WT controls (Fig. 1 B). We also found that type 2 ATMs in lean mice from both genotypes express ST2 (Fig. 1 C), a member of the TLR-IL receptor superfamily that negatively regulates TLR4 signaling (Brint et al., 2004). Similar to MGL1, ST2 expression is restricted to type 2 ATMs in interstitial spaces of adipose tissue from obese mice and is not expressed in inflammatory type 1 ATMs in CLS (Isolectin$^+$; Fig. 1 D). MGL1 staining confirmed the lack of MGL1 expression in *Mgl1*$^{-/-}$ mice, and demonstrated specificity of the antibody for MGL1 (Fig. 1 C). Overall, these results demonstrate that MGL1 is not required for the proper localization and antiinflammatory characteristics of resident type 2 ATMs.

High-fat diet (HFD)-fed *Mgl1*$^{-/-}$ mice show slight protection from DIO by HFD feeding

Although MGL1 does not influence the phenotype of resident ATMs in lean mice, we hypothesized that *Mgl1* deficiency might alter inflammation and insulin resistance in the context of DIO. Therefore, we placed *Mgl1*$^{-/-}$ and control mice on a HFD for 18 wk. *Mgl1*$^{-/-}$ mice gained weight at a similar rate as WT controls until the last weeks of the HFD feeding when the weight of *Mgl1*$^{-/-}$ mice was slightly reduced compared with controls (Fig. 2 A). There were no differences in weight

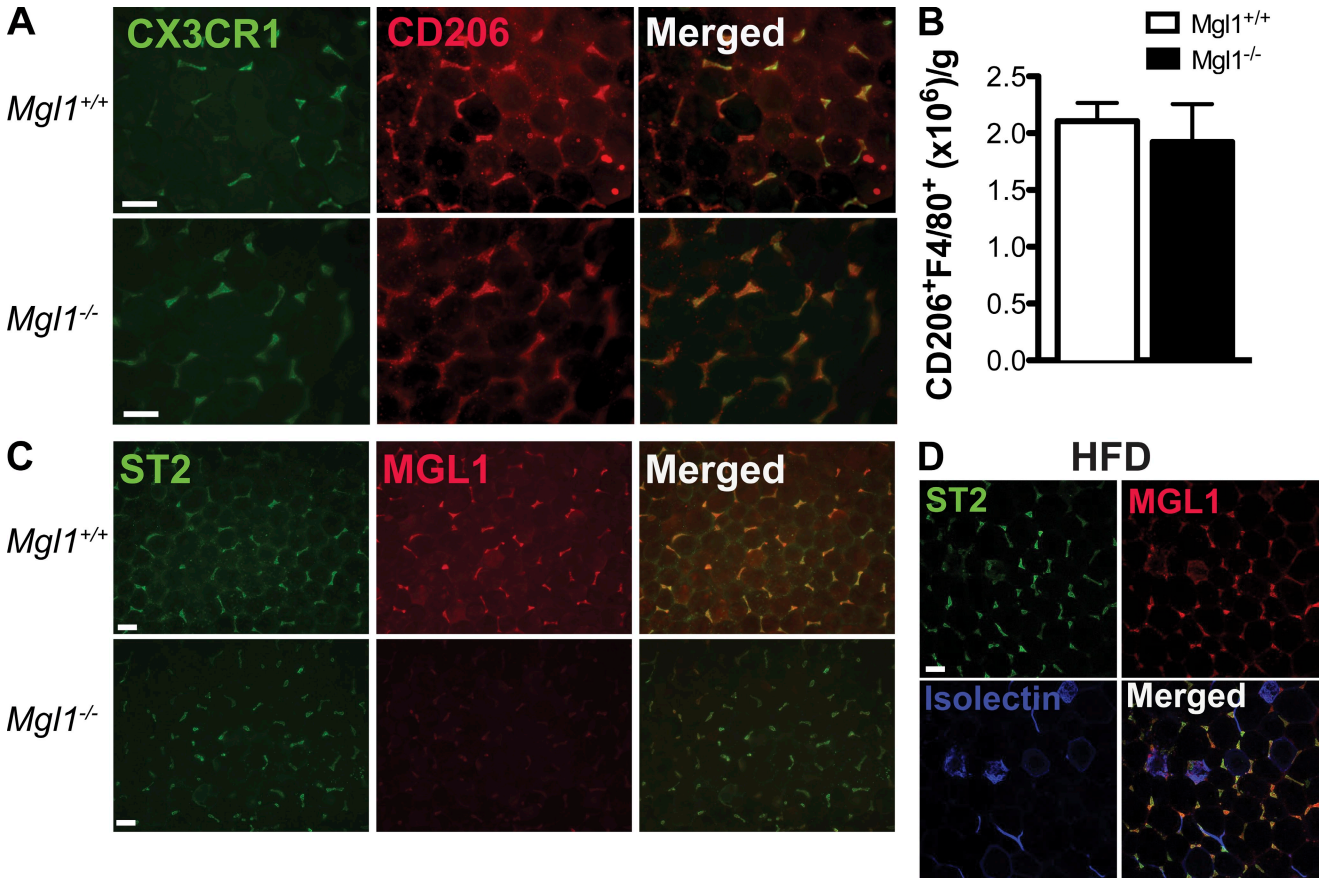

Figure 1. Type 2 ATMs are unchanged in lean Mgl1$^{-/-}$ mice. (A) Analysis of ATMs in lean mice for markers of alternative activation. Epididymal white adipose tissue (EWAT) from lean *Mgl1*$^{-/-}$ and *Mgl1*$^{+/+}$ mice were stained for CD206 and CX3CR1. (B) Quantitation of F4/80^{+} CD206^{+} ATMs in lean *Mgl1*$^{-/-}$ and *Mgl1*$^{+/+}$ mice. SVF isolated from EWAT ($n = 4$) and analyzed by flow cytometry. Total ATM numbers were normalized to tissue mass. (C) ST2 expression in type 2 resident ATMs. EWAT from ND-fed *Mgl1*$^{-/-}$ and control C57BL/6 mice were stained for ST2 (green) and MGL1 (red). Staining and imaging parameters were identical between samples to demonstrate the specificity of the antibodies for MGL1. (D) ST2 expression in obese mice. Isolectin staining identifies CLSs containing type 1 ATM clusters. Samples from EWAT from HFD-fed C57BL/6 mice. (A, C, and D) Representative images shown from one of at least three independent experiments. Bars, 50 µm.

between ND-fed *Mgl1*$^{-/-}$ and *Mgl1*$^{+/+}$ mice (Fig. 2 B). No significant difference in food intake was observed between *Mgl1*$^{-/-}$ mice and control mice that could explain the slight weight difference (Fig. 2 C). Respiratory quotient was also similar between the two genotypes (Figs. 2 D). A small, but statistically significant increase in oxygen consumption was seen in HFD-fed *Mgl1*$^{-/-}$ mice, but this lost significance when corrected for lean body mass (Fig. 2 E).

Body composition analysis showed that HFD-fed *Mgl1*$^{-/-}$ mice had less fat mass compared with controls, and this primarily accounted for the difference in weight (Fig. 2 F). Examination of the tissue weights showed that *Mgl1*$^{-/-}$ mice had less subcutaneous white adipose tissue (inguinal fat pad) and lower liver weight. When expressed as a percentage of total body weight, liver weight was significantly decreased in *Mgl1*$^{-/-}$ mice. Surprisingly, obese *Mgl1*$^{-/-}$ mice had a different distribution of fat, with relatively more visceral white adipose tissue (epididymal fat pad) than HFD-fed control mice (Fig. 2 G). Overall, *Mgl1*$^{-/-}$ mice showed slight protection from long-term HFD feeding, but had a greater accumulation of visceral fat compared with controls.

MGL1 plays a role in DIO-induced insulin resistance and glucose intolerance

Glucose metabolism was evaluated in ND and HFD-fed *Mgl1*$^{-/-}$ and WT mice. HFD-fed mice from both genotypes demonstrated fasting hyperglycemia compared with ND-fed mice, and there were no significant differences between genotypes (Fig. 3 A). Fasting insulin levels were elevated in HFD-fed mice compared with lean controls with a trend toward increased insulin levels in knockout versus WT controls (Fig. 3 B; $P = 0.2$). Glucose tolerance tests showed no differences between lean ND-fed *Mgl1*$^{-/-}$ and controls (Fig. 3 C). However, obese *Mgl1*$^{-/-}$ mice had significantly improved glucose tolerance compared with HFD-fed controls. Insulin tolerance tests demonstrated that HFD *Mgl1*$^{-/-}$ mice were significantly more insulin sensitive than obese *Mgl1*$^{+/+}$ mice with a profile similar to ND mice (Fig. 3 D). These data show

that *Mgl1*$^{-/-}$ deficiency leads to improved glucose tolerance and insulin sensitivity with DIO.

The protection from insulin resistance in *Mgl1*$^{-/-}$ mice occurred in spite of the fact that *Mgl1*$^{-/-}$ mice have proportionately more visceral fat. Examination of visceral adipose tissue showed that obese *Mgl1*$^{-/-}$ had more intact adipocytes and fewer macrophage-containing CLS compared with HFD-fed *Mgl1*$^{+/+}$ controls (Fig. 3 E). Analysis of adipocyte size demonstrated that obese *Mgl1*$^{-/-}$ mice had significantly larger adipocytes compared with obese controls (Fig. 3 F). Overall, the data showed that HFD-fed *Mgl1*$^{-/-}$ mice had more visceral fat than controls correlating with more extensive adipocyte hypertrophy and less ATM accumulation.

These observations suggested that *Mgl1*$^{-/-}$ mice are more efficient at storing lipid in adipose tissue with HFD. Analysis of serum-free fatty acid (FFA) levels confirmed that *Mgl1*$^{-/-}$ mice had lower circulating levels of FFAs than obese controls (Fig. 3 G). Furthermore, liver histology demonstrated that *Mgl1*$^{-/-}$ mice were protected from hepatic steatosis induced by HFD feeding, a finding that likely explains the difference in liver mass between the genotypes (Fig. 3 H). Overall, this demonstrates that obese *Mgl1*$^{-/-}$ mice have more efficient

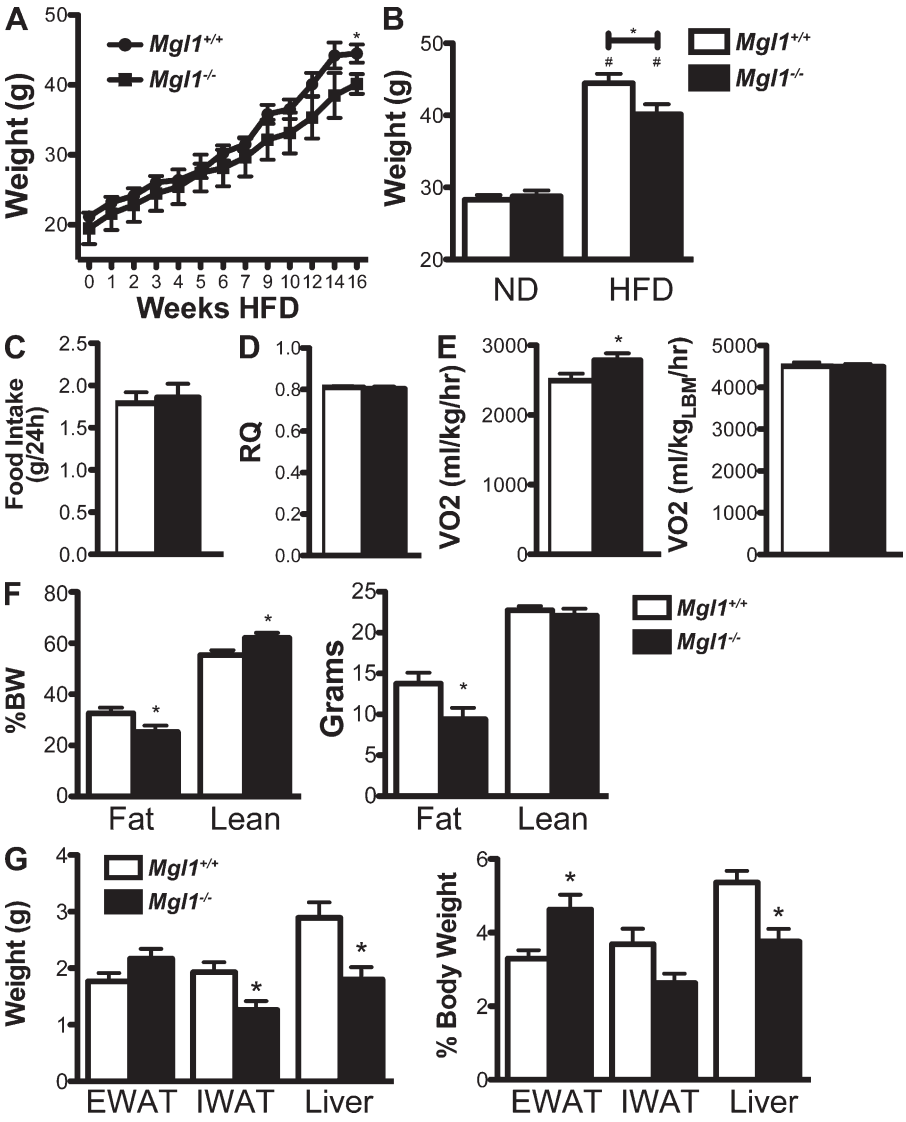

Figure 2. Effect of DIO on *Mgl1*$^{-/-}$ mice. (A) Weight gain in HFD-fed *Mgl1*$^{-/-}$ and control mice. Mice fed a diet of 60% kcal from fat. *, $P < 0.05$. $n = 6$ per genotype. (B) Total body weights of ND and HFD-fed mice. *, $P = 0.049$; #, $P < 0.0001$ versus ND. $n = 10$ mice per group. (C–F) Metabolic parameters of HFD-fed mice. *, $P < 0.05$. $n = 6$ per group. CLAMS unit used to measure food intake (C), respiratory quotient (D), and oxygen consumption (E) in HFD-fed mice. VO2 data shown with and without normalization for lean body weight (LBW). (F) Body composition analysis of HFD-fed mice measured with MRI and corrected for body weight. (G) Tissue weights in HFD-fed mice. Tissue weight with and without normalization to total body weight is presented. *, $P < 0.05$ versus WT. $n = 9$ mice per genotype. Results combined from 2 independent sets of animals.

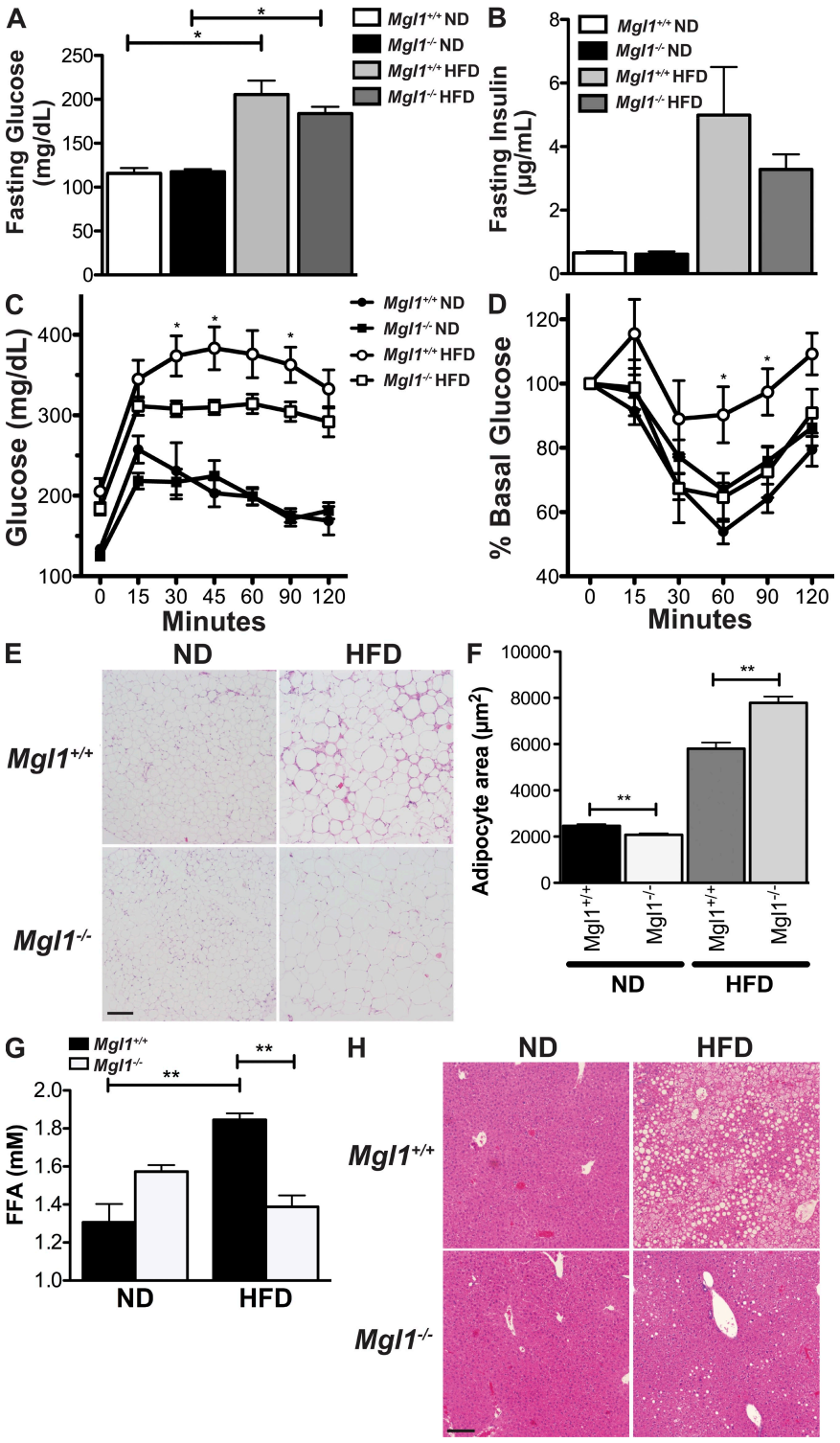

Figure 3. ***Mgl1*$^{-/-}$ mice are protected from DIO-induced insulin resistance.** Fasting glucose levels (A) and insulin levels (B). *, $P < 0.05$. $n = 9–12$ per group. (C) Glucose tolerance test. Glucose levels were measured after i.p. injection of 0.7 g/kg glucose. *, $P < 0.05$ versus *Mgl1*$^{+/+}$. $n = 10$ per group from two independent experiments. (D) Insulin tolerance test. Glucose levels were measured after i.p. injection of 1 U/kg insulin. *, $P < 0.05$ versus *Mgl1*$^{+/+}$. $n = 6$ per group from two independent experiments. (E) Hematoxylin and eosin (H&E)–stained sections from epididymal adipose tissue from mice. Representative images shown. Similar results seen in four independent samples. (F) Adipocyte sizing from visceral adipose tissue. Adipocyte cross-sectional area was assessed on H&E sections by analysis of 150 adipocytes per mouse from 3 separate sections and 3–4 mice per group. **, $P < 0.0001$. (G) FFA levels. Fasting serum was collected and analyzed for nonesterified FFA levels. **, $P < 0.0001$. $n = 6–8$ mice per group. (H) H&E-stained sections from liver biopsies from mice. Representative images shown. Similar results seen in four independent samples.

lipid storage in adipose tissue compared with controls, thus providing protection from fatty liver.

Mgl1 is required for the accumulation of proinflammatory type 1 ATMs with DIO

The adipose tissue histology suggested that alterations in ATM-induced inflammation might explain the protection from insulin resistance in obese *Mgl1*$^{-/-}$ mice. Examination of inflammatory gene expression in epididymal adipose tissue showed that obese *Mgl1*$^{-/-}$ mice had significantly more *Il10* expression compared with controls (Fig. 4 A). *Il10* expression was not altered in the inguinal fat pads from the *Mgl1*$^{-/-}$ mice, suggesting that *Mgl1* deficiency primarily effects visceral fat inflammation. No other significant differences in inflammatory gene expression were seen between genotypes, although there was a trend toward a decrease in *Itgax/Cd11c* expression and an increase in *Cx3cr1* expression in *Mgl1*$^{-/-}$ mice. *Mgl2* expression was not changed in adipose tissue with *Mgl1* deficiency, demonstrating that this orthologue is not up-regulated to compensate for the lack of MGL1. No significant differences in gene expression were seen in inguinal (subcutaneous) fat (Fig. 4 B).

Because type 2 ATMs are a source of IL-10 in adipose tissue (Lumeng et al., 2008), we hypothesized that obese *Mgl1*$^{-/-}$ mice may have an altered ratio of type 1 to type 2 ATMs. To test this, we evaluated ATM content in obese mice by flow cytometry using markers of type 1 (CD11c) and type 2 (CD206) ATMs (Fig. 4 C; Nguyen et al., 2007). Although the percentage of F4/80$^+$ CD11b$^+$ ATMs in *Mgl1*$^{-/-}$ mice was similar to controls, the total number of ATMs isolated from epididymal fat pads was slightly decreased. The content of CD11c$^+$ ATMs in obese *Mgl1*$^{-/-}$ mice was reduced to ∼40% of WT levels that persisted with normalization to fat weight. This resulted in an overall reduction in the ratio of type 1 to type 2 (CD11c$^+$/CD206$^+$) ATMs in HFD-fed *Mgl1*$^{-/-}$ mice (Fig. 4 D). CD206 staining was not different between ATMs from *Mgl1*$^{-/-}$ mice and controls, demonstrating that the expression of this lectin is also not altered in the absence of MGL1.

Immunofluorescence microscopy of epididymal fat pads supported the flow cytometry data. There was a significant decrease in the number of type 1 ATM clusters in fat from *Mgl1*$^{-/-}$ mice compared with *Mgl1*$^{+/+}$ controls (Fig. 4 E). This protection from type 1 ATM accumulation was more striking with long-term HFD exposure (26 wk) as *Mgl1*$^{-/-}$ mice had very few Mac2$^+$ CLS compared with controls (Fig. 4 F). Composite images demonstrated that CLS were not uniformly distributed in epididymal fat pads in HFD-fed WT mice.

To evaluate the effects of MGL1 deficiency on systemic inflammation in obesity, we examined serum cytokine levels in the mice (Fig. 4 G). Inflammatory cytokines RANTES/CCL5 and TNF were increased with HFD in control mice. However, the levels of these chemokines were decreased in HFD *Mgl1*$^{-/-}$ mice compared with controls. IL-10 was similarly decreased in *Mgl1*$^{-/-}$ mice consistent with previous observations (Saba et al., 2009). CCL2/MCP-1 levels were increased in HFD-fed *Mgl1*$^{-/-}$ mice compared with controls. Overall, our data suggest that the improved glucose and insulin tolerance in *Mgl1*$^{-/-}$ mice is related to a decrease in the accumulation of type 1 inflammatory ATMs in visceral adipose tissue, less adipose tissue inflammation, less systemic inflammation, and more intact adipocytes, which led to less hepatic steatosis.

7/4^{hi} inflammatory monocytes express MGL1 and are not induced by DIO in *Mgl1*$^{-/-}$ mice

The prior results were unexpected, as it appeared that MGL1 was required for the accumulation of type 1 ATMs with low MGL1 expression. Additionally, despite elevated levels of CCL2 in obese *Mgl1*$^{-/-}$ mice, ATM trafficking to fat was not increased and was, in fact, suppressed. We hypothesized that these observations might relate to an undescribed role for MGL1 in monocytes in the bone marrow or blood that give rise to ATMs. To evaluate this, we examined the quantity of 7/4^{hi} and 7/4^{mid} monocytes, monocyte subclasses with different inflammatory functions, in the blood of *Mgl1*$^{-/-}$ and *Mgl1*$^{+/+}$ mice on different diets (Fig. 5 A). In ND mice, *Mgl1*$^{-/-}$ mice had similar amounts of 7/4^{hi} monocytes compared with controls, but had an increased percentage of 7/4^{mid} monocytes in the blood. Similar to other studies (Tsou et al., 2007), we observed an increase in circulating 7/4^{hi} monocytes in control mice with HFD. However, in *Mgl1*$^{-/-}$ mice, DIO did not induce an increase in 7/4^{hi} inflammatory monocytes. 7/4^{mid} monocytes were not significantly different between HFD-fed *Mgl1*$^{-/-}$ and control mice. Examination of 7/4^{hi} and 7/4^{mid} monocytes in the bone marrow demonstrated no significant differences in the monocyte subclasses between *Mgl1*$^{-/-}$ and control mice (Fig. 5 B).

These results suggest that MGL1 plays a role in the induction and/or maintenance of circulating 7/4^{hi} monocytes in response to DIO that ultimately attenuates the accumulation of type 1 inflammatory ATMs. Consistent with this, we found that MGL1 was expressed only on 7/4^{hi} monocytes and not on 7/4^{mid} monocytes in lean animals (Fig. 5, C and D). HFD exposure induced low MGL1 expression in 7/4^{mid} monocytes.

Mgl1 regulates monocyte half-life in the circulation and is required for maximal macrophage recruitment to sites of inflammation

The identification of MGL1 expression on monocytes suggests that MGL1 deficiency alters the properties of circulating monocytes. This would provide a mechanism to explain the decrease in 7/4^{hi} monocytes in the blood, but not the bone marrow, of knockout mice. It can also explain the attenuation of ATM accumulation in visceral fat despite adipocyte hypertrophy. To assess this, we performed adoptive transfer experiments to compare the circulating half-life of monocytes from wild-type and *Mgl1*$^{-/-}$ mice. CFSE-labeled monocytes from the two genotypes were injected IV into C57BL/6 recipients and circulating CD11b$^+$ monocytes were quantified in the blood 24 and 72 h after injection. This demonstrated that fewer monocytes were recovered from the circulation after transfer of *Mgl1*$^{-/-}$ cells compared with control cells at

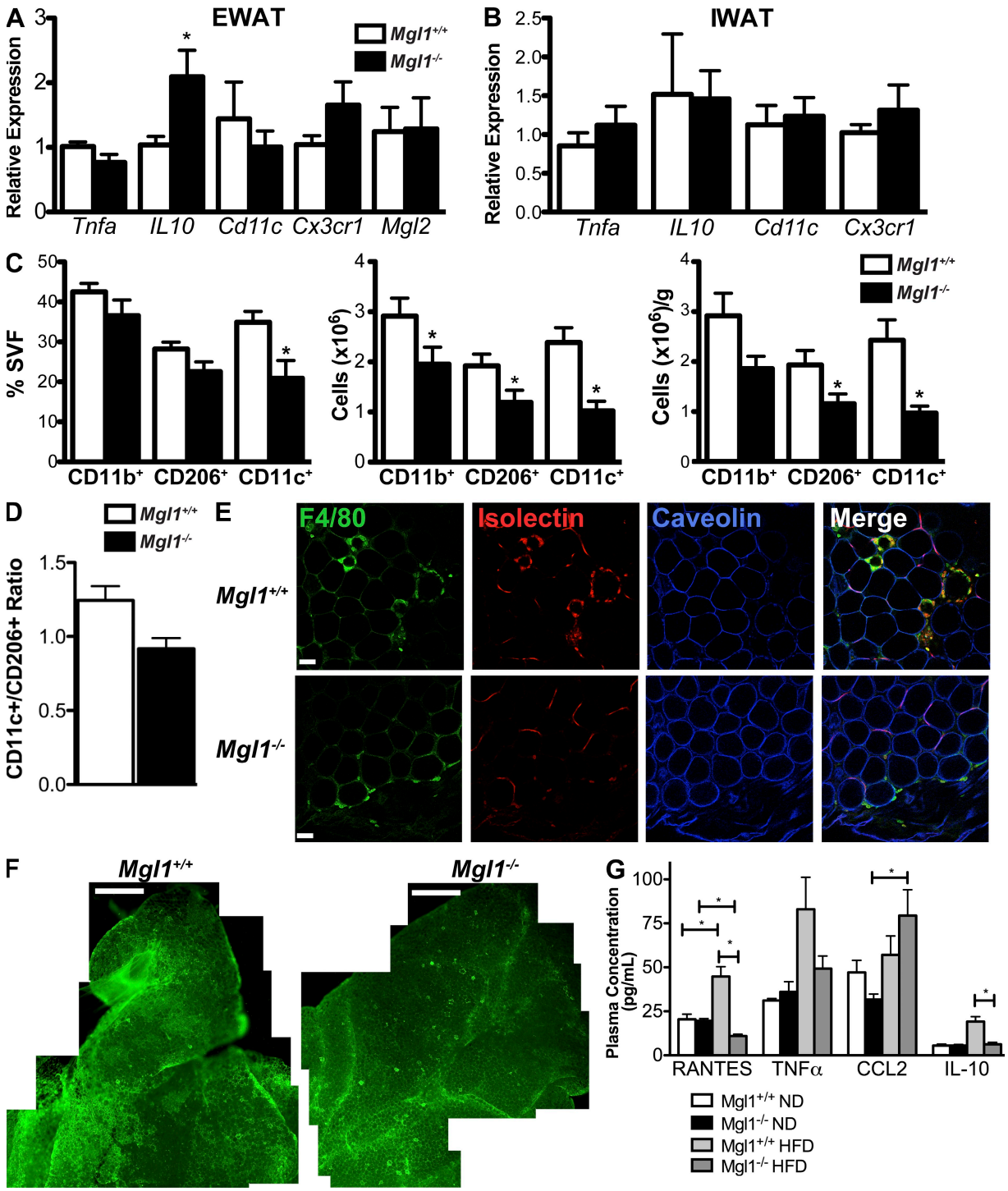

Figure 4. ***Mgl1*$^{-/-}$ mice have fewer type 1 CD11c^{+} ATMs and decreased adipose tissue inflammation with DIO.** (A and B) Expression analysis of inflammatory genes in adipose tissue from HFD-fed *Mgl1*$^{-/-}$ and WT mice. Samples from epididymal (EWAT; A) and inguinal (IWAT; B) fat analyzed by real-time quantitative RT-PCR. *, $P < 0.05$ versus *Mgl1*$^{+/+}$. $n = 4$ per group. (C) ATM content assessed by flow cytometry in HFD-fed *Mgl1*$^{-/-}$ and WT mice. SVF cells obtained from EWAT from HFD-fed mice. Cells gated for F4/80^{+} ATMs and analyzed for expression of markers of type 1 (CD11c) and type 2 (CD206) ATMs. Data shown as percentage of SVF, total cells, and normalized to tissue weight. *, $P < 0.05$ vs *Mgl1*$^{+/+}$. $n = 6$ per group. (D) Ratio of CD11c^{+} (type 1) ATMs to CD206^{+} (type 2) ATMs. (E) Confocal microscopy of adipose tissue from HFD-fed *Mgl1*$^{-/-}$ and control mice. Caveolin staining identifies intact adipocytes. Isolectin identifies CLSs and vasculature. Samples from EWAT. Bars, 50 µm. (F) Composite images from tips of EWAT fat pads stained for Mac2^{+} ATMs. Bars, 500 µm. (G) Plasma cytokine analysis from HFD-fed *Mgl1*$^{-/-}$ and WT mice. $n = 6$ mice per group. **, $P < 0.05$. Samples combined from two independent sets of mice.

both time points (Fig. 6 A). Assessment of transferred cells in the spleen at 72 h showed equal numbers of monocytes and did not suggest that sequestration in the spleen explained the peripheral monocyte phenotype (unpublished data). This suggests that *Mgl1* deficiency alters the intrinsic properties of monocytes that helps maintain them in the circulation.

To further assess the importance of MGL1 in promoting monocyte trafficking to inflammatory sites, we looked at the accumulation of thioglycollate (TG)-elicited peritoneal macrophages (PMs) in $Mgl1^{-/-}$ mice. TGPMs had increased MGL1 expression compared with resident PMs, consistent with other reports of MGL1 induction upon stimulation of migration (Fig. 6 B; Dupasquier et al., 2006). Analysis of the accumulation of PMs after TG injection showed that $Mgl1^{-/-}$ mice had fewer cells recruited 18 h after injection compared with WT controls (Fig. 6 C). At the 72 h time point, there was no significant difference between the two genotypes. $Ccr2^{-/-}$ controls showed little PM recruitment after TG injection. In addition, TG-elicited PMs from $Mgl1^{-/-}$ mice had decreased TNF expression with LPS treatment compared with controls,

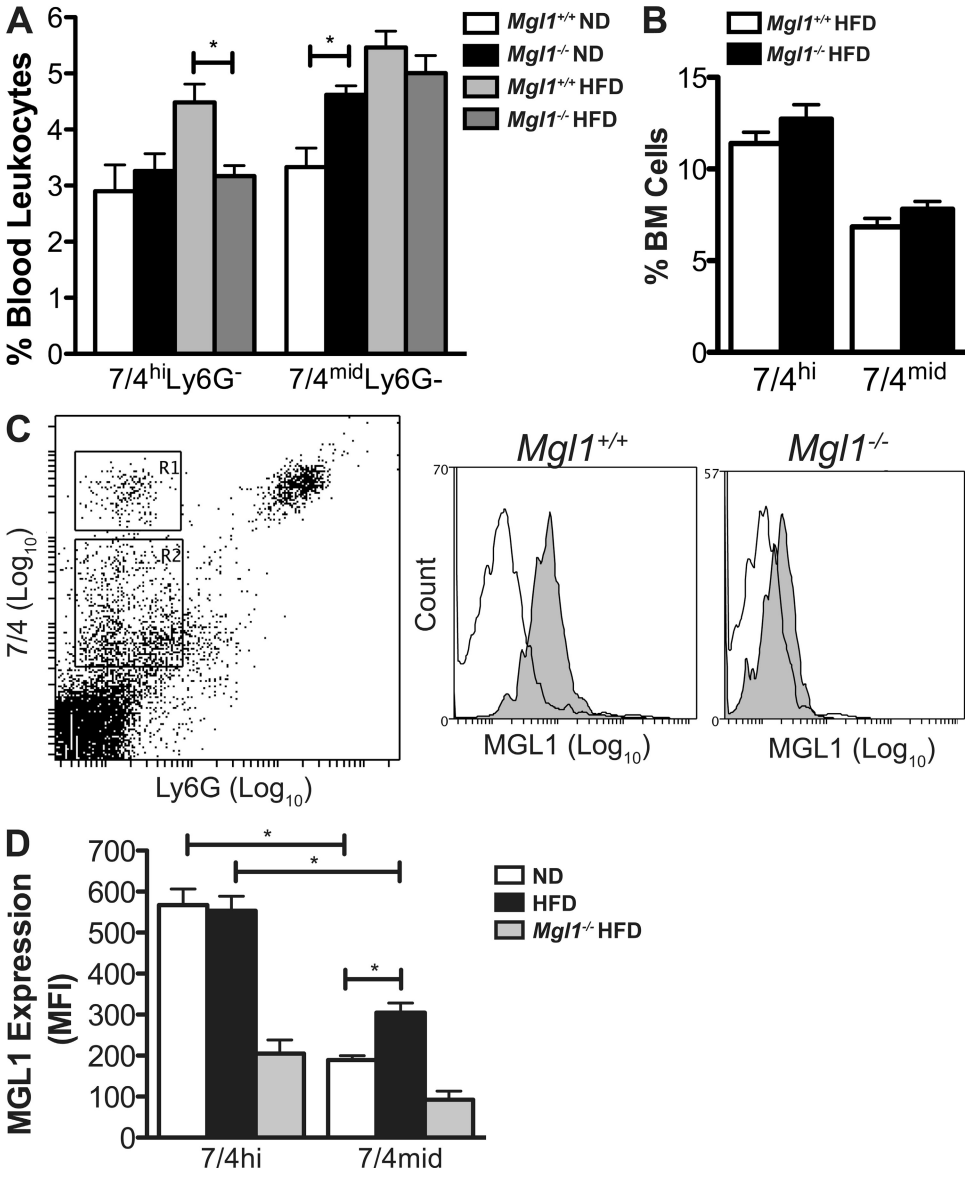

Figure 5. MGL1 is expressed on and regulates levels of 7/4^{hi} blood monocytes. (A) Quantitation of 7/4^{hi} and 7/4^{mid} monocytes in blood from ND and HFD-fed $Mgl1^{-/-}$ and control mice by flow cytometry. n = 12 mice per group. (B) Quantitation of 7/4^{hi} and 7/4^{mid} monocytes in BM from HFD-fed $Mgl1^{-/-}$ and control mice by flow cytometry. n = 6 mice per group. (C) MGL1 expression in 7/4^{hi} inflammatory monocytes. Flow cytometry performed on blood from male mice. 7/4^{hi} Ly6G^{-} inflammatory monocytes (R1, gray) and 7/4^{mid} Ly6G^{-} (R2, white) were gated and analyzed for MGL1 expression. Representative plot shown from five independent experiments. (D) MGL1 expression in blood monocytes with HFD-induced obesity. MFI of MGL1 staining for monocyte subtypes in ND and HFD-fed C57BL/6 mice. Staining of $Mgl1^{-/-}$ monocytes shows antibody specificity. n = 4 mice per group. *, $P < 0.05$. Data are representative of data combined from two to three independent sets of animals.

suggesting that the recruited *Mgl1*$^{-/-}$ PM have less inflammatory potential (Fig. 6 D). Overall, these results support a role for MGL1 in generating the maximal recruitment of inflammatory mononuclear phagocytes to sites of inflammation.

Mgl1$^{-/-}$ monocytes demonstrate decreased adhesion to adipocytes in vitro and Lewis X is up-regulated in fat with DIO

Another property of monocytes that might explain the protection from ATM infiltration is altered interactions between adipocytes and MGL1-deficient monocytes. To assess this hypothesis, we compared the adhesion of monocytes from control and *Mgl1*$^{-/-}$ mice to 3T3-L1 adipocytes, a well established adipocyte cell line. In this assay, the adhesion of *Mgl1*$^{-/-}$ monocytes was significantly decreased compared with wild type (Fig. 7 A). This difference was not seen when monocytes were incubated with an endothelial cell line (bEnd.3) in the presence or absence of TNF (Fig. 7 B). This suggests that ligands for MGL1 are present on adipocytes and may regulate the trafficking and/or retention of macrophages or monocytes in adipose tissue.

MGL1 binds Lewis X trisaccharides with high-affinity and specificity (Singh et al., 2009). This led us to hypothesize that the DIO would induce or alter the expression of Lewis X motifs in adipose tissue that might direct the trafficking of MGL1^{+} 7/4^{hi} monocytes. Lewis X was not detected in visceral adipose tissue from lean mice (Fig. 7 C). However, in obese mice, Lewis X was detected as highly concentrated in the isolectin^{+} CLS (Fig. 7 D). This indicates that MGL1 binding targets are induced in CLS with DIO, which may play a role in 7/4^{hi} monocyte trafficking to these regions.

DISCUSSION

Our study reveals a novel and unexpected function for the murine scavenger receptor MGL1 in the regulation of the inflammatory response to obesity. Because MGL1 is highly expressed in type 2 ATMs that secrete IL-10 and have low inflammatory activity, our initial hypothesis was that *Mgl1* knockout mice would have a higher ratio of type 1 ATMs to type 2 ATMs, and thus more inflammation. Surprisingly, we found that *Mgl1*$^{-/-}$ mice are protected from HFD-induced insulin resistance and steatosis, which correlates with attenuation of inflammatory ATM accumulation in visceral fat despite having larger adipocytes. The mechanism behind this phenotype is related to the observation that MGL1 regulates the properties of circulating monocytes that ultimately impact the appearance of ATMs in fat. MGL1 is expressed on inflammatory 7/4^{hi} monocytes in the blood, a suspected precursor of type 1 ATMs, and these cells are decreased in the circulation of obese animals. The absence of MGL1 alters the

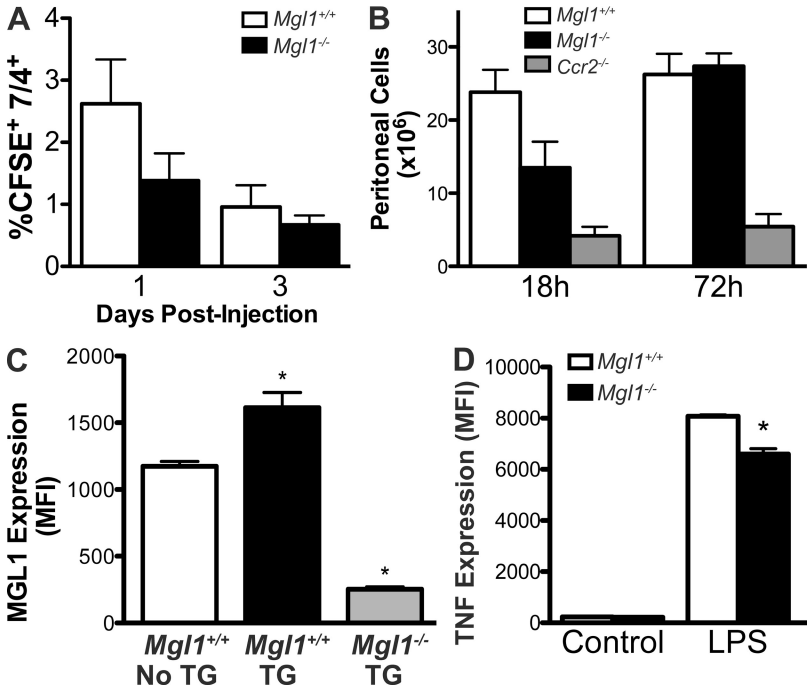

Figure 6. Decreased inflammatory activity in *Mgl1*$^{-/-}$ PMs. (A) Decreased half-life of *Mgl1*$^{-/-}$ monocytes after adoptive transfer. Circulating CD11b^{+} monocytes were quantified in the blood 1 and 3 d after i.v. injection of 2 × 10^{6} CFSE-labeled monocytes into C57BL/6 mice. *n* = 9 per group. (B) Quantitation of PMs after injection in *Mgl1*$^{-/-}$ and control mice. Peritoneal cells were assessed 18 and 72 h after i.p. TG injection into *Mgl1*$^{-/-}$, *Ccr2*$^{-/-}$, and control mice. *n* = 4 mice per group. (C) MGL1 expression on TG elicited PMs. Flow cytometry for MGL1 expression on PMs isolated from mice with and without TG injection. Expression presented as MFI of MGL1 expression in F4/80^{+} cells. *n* = 4 per group. (D) TNF expression in macrophages from *Mgl1*$^{-/-}$ and control mice. PMs were isolated from mice and stimulated with or without 0.1 µg/ml LPS in complete media for 6 h. Cells were stained for intracellular TNF expression and quantitated by MFI. *n* = 4 per group. All data were observed in two independent experiments.

properties of these monocytes decreasing their survival in the circulation. MGL1 also participates in mediating the adhesion between monocytes and adipocytes, and we have identified Lewis X binding sites for MGL1 that are increased in adipose tissue with DIO.

These observations demonstrate that MGL1 is among a growing number of leukocyte receptors and chemokines that regulate the appearance and stability of monocytes in the circulation. CX_3CR1 regulates $7/4^{mid}$ $Gr\text{-}1^{lo}$ monocyte numbers in mice by enhancing their survival in the circulation (Landsman et al., 2009). CCR2 is now recognized to be critical for the migration of monocytes from the bone marrow into the circulation via interactions with CCL2/MCP-1 and CCL7/MCP-3 (Serbina and Pamer, 2006; Tsou et al., 2007). *Ccr2*$^{-/-}$ mice have a profound loss of $7/4^{hi}$ $Ly6c^{+}$ monocytes with preservation of circulating $7/4^{mid}$ monocytes in the blood (Tsou et al., 2007). This translates into a lack of accumulation of type 1 ATMs in obese *Ccr2*$^{-/-}$ mice, the normal recruitment of type 2 ATMs, and protection from obesity-induced insulin resistance (Weisberg et al., 2006; Lumeng et al., 2007b, 2008).

Both obese *Mgl1*$^{-/-}$ mice and *Ccr2*$^{-/-}$ mice demonstrate that attenuation of inflammatory $7/4^{hi}$ $Ly6c^{+}$ monocytes can block ATM accumulation in adipose tissue, decrease

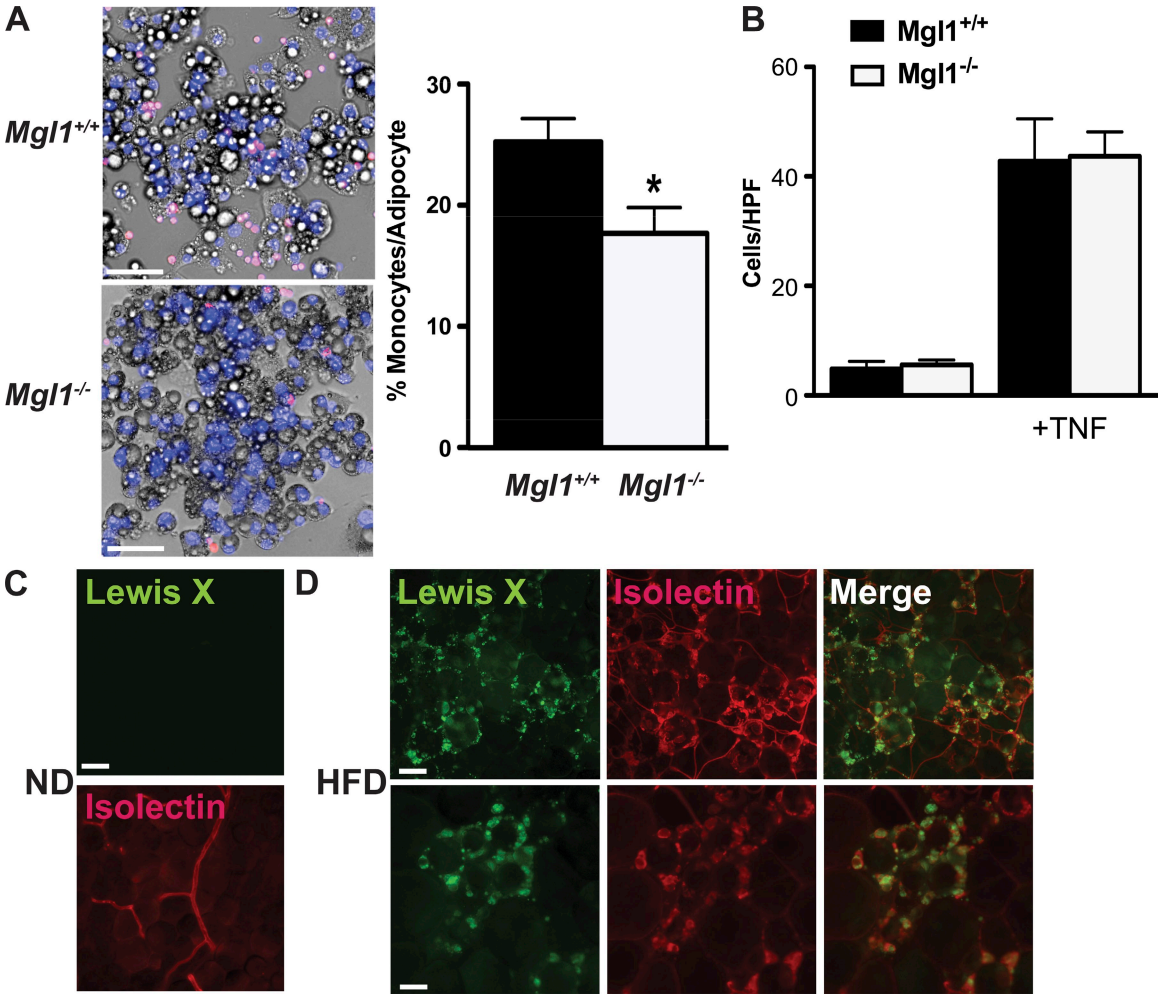

Figure 7. MGL1 regulates monocyte adhesion to adipocytes. (A) Monocytes from *Mgl1*$^{-/-}$ mice have decreased adhesion to adipocytes. 0.5×10^6 CFSE-labeled monocytes were incubated with differentiated 3T3-L1 adipocytes for 30 min. After extensive washing to remove nonadherent cells, wells were fixed and stained with DAPI (blue). Images were analyzed by quantifying $CFSE^{+}$ cells (pink) that were attached to adipocytes and normalizing this number to the number of adipocytes per high-power field. Eight images were analyzed from four independent experiments. *, $P < 0.05$. (B) *Mgl1*$^{-/-}$ monocytes have normal adhesion to endothelial cells. After treatment of bEnd.3 monolayers with or without TNF (50 ng/ml), 0.5×10^6 CFSE-labeled monocyte were added to the wells. After 30 min, cells were washed and fixed. Adherent CFSE cells were quantitated by imaging at 200×. Two images were analyzed from each of eight independent samples, and the experiment was repeated twice. (C) Lewis X is not detected in epididymal adipose tissue from lean ND-fed mice. Epididymal fat pads from ND-fed C57BL/6 mice were stained with anti-Lewis X antibodies and isolectin to identify blood vessels. (D) Lewis X is highly expressed in CLS in visceral adipose tissue from obese HFD-fed mice. Epididymal fat pads from HFD-fed C57BL/6 mice were stained with anti-Lewis X antibodies and isolectin to identify blood vessels. Representative images are shown. Similar results were obtained from three independent samples. Bars, 50 µm.

obesity-induced inflammation in fat, and improve glucose tolerance. These observations provide added support to a model where differential trafficking of monocyte subpopulations generates the increased ratio of type 1 to type 2 and the "phenotypic switch" to a proinflammatory environment with obesity. Our results suggest that a critical nexus of interaction between obesity and inflammation may reside at the level of circulating monocytes, and support the results of other studies showing activation of peripheral monocytes in obesity (Ghanim et al., 2004; Degasperi et al., 2009). This perspective suggests that the elevations in circulating CCL2/MCP-1 seen in obesity and type 2 diabetes (Sartipy and Loskutoff, 2003; Takahashi et al., 2003) may in fact play a primary role in promoting egress of inflammatory monocytes from the bone marrow into the circulation, rather than just the recruitment of these cells from the circulation into adipose tissue. Redundant signals from CCL2 and CCL7 to promote the migration of $CCR2^+$ monocytes from the bone marrow could explain why examination of ATMs in obese *Ccl2*$^{-/-}$ mice has led to variable results (Kanda et al., 2006; Inouye et al., 2007; Kirk et al., 2008).

Evaluation of glucose metabolism in obese *Mgl1*$^{-/-}$ mice demonstrates a significant protection from insulin resistance and type 1 ATM accumulation that is out of proportion to the modest difference in body weight observed. It is possible that differences in glucose metabolism observed are caused by the slight weight loss seen in the *Mgl1*$^{-/-}$ mice. However, *Mgl1*$^{-/-}$ mice actually have more visceral adipose tissue than controls with DIO, which is partially caused by larger adipocytes. The unique dissociation between adiposity and glucose intolerance is associated with a profound lack of ATM infiltration in *Mgl1*$^{-/-}$ mice, further supporting a primary role for ATMs in the regulation of glucose metabolism. The deficiency of type 1 ATMs in the knockout mice results in more intact adipocytes, improved triglyceride storage in fat, decreased circulating FFA, and protection from hepatic steatosis.

These observations emphasize a property of adipose tissue that is still poorly understood: how visceral adipose tissue expansion may actually be metabolically beneficial in certain contexts. This agrees with recent observations that overexpression of adiponectin in leptin-deficient animals led to adipose tissue expansion without inflammation and maintained insulin sensitivity despite profound obesity (Kim et al., 2007).

Composite images (Fig. 4 F) demonstrate that the ATM accumulation with DIO is not uniform as CLS are distributed in patches. This regional variation in ATM accumulation may explain the variation in RT-PCR analysis of gene expression in small fat biopsy samples. Our observation of increased IL-10 expression and a decrease in the ratio of type 1 to type 2 ATMs in visceral fat from obese *Mgl1*$^{-/-}$ mice provides further support for the idea that ATM activation state is an important variable in the generation of adipose tissue inflammation. Changes in IL-10 were not observed in subcutaneous fat in the knockout animals which may be caused by the fact that type 1 ATMs do not accumulate in this depot as significantly as in visceral fat (Lumeng et al., 2007b). Such differences may also be caused by other sources of IL-10 such as newly identified adipose tissue regulatory T cells (Feuerer et al., 2009).

We also found that MGL1-deficient monocytes had decreased adhesion to adipocytes in vitro which can contribute to the significant decrease in type 1 ATM accumulation in obese *Mgl1*$^{-/-}$ mice. Less efficient binding of the *Mgl1*$^{-/-}$ $7/4^{hi}$ monocytes to adipocytes may work in concert with their lower levels to attenuate inflammation. Although glycan arrays have shown that MGL1 binds to Lewis X and Lewis A trisaccharides, the full range of binding partners in vivo has yet to be revealed. We speculated that DIO and hyperglycemia promote the formation of a Lewis X containing ligands for MGL1 and observed the induction of Lewis X expression in CLS with DIO, an observation that may provide a means for circulating $MGL1^+$ $7/4^{hi}$ monocytes to traffic to CLS.

We did not find evidence that other lectin receptors such as MGL2 or CD206 are up-regulated in macrophages in response to MGL1 deficiency. Human MGL promotes interactions between DCs and endothelial cells that inhibit migration and promote retention of DCs in lymphoid organs (van Vliet et al., 2008b). Glycosylation-dependent interactions between leukocytes and endothelial cells play a significant role in the recruitment of inflammatory cells to atherosclerotic plaques via interactions between PSGL-1 and P-selectin (Lowe, 2003; Martinez et al., 2005). Our observations with Lewis X are consistent with these observations, and the report of alterations in glycosylation at Lewis X residues on α1-acid glycoprotein in type I diabetes (Poland et al., 2001). Further studies will be needed to assess if mMGL1, mMGL2, or hMGL are potential targets for inhibitors that could specifically target the obesity-induced trafficking of inflammatory monocytes and attenuate the formation of type 1 ATMs.

We have identified ST2 as a novel marker of type 2 ATMs. The expression of this receptor can inhibit signaling from TLR receptors suggesting another mechanism by which type 2 ATMs maintain a suppressed inflammatory state. Lack of ST2 in type 1 ATMs may help maintain proinflammatory signals from TLR4 activated by free fatty acids that are concentrated in adipose tissue (Shi et al., 2006; Nguyen et al., 2007; Coenen et al., 2009).

We have previously referred to ATM subtypes as M1 and M2 ATMs; however, this is imprecise and likely overly simplistic because these states were defined in vitro (Gordon and Taylor, 2005). Additionally, how the "M1/M2 paradigm" relates to human macrophages is still unclear (Zeyda et al., 2007; Bourlier et al., 2008). We propose a new nomenclature for these ATM subtypes: type 1 ATMs are $F4/80^+$ $MGL1^-$ $CD206^-$ $ST2^-$ $CD11c^+$ and are concentrated in CLS. These ATMs express many genes seen in classically activated M1 macrophages. Type 2 ATMs are $F4/80^+$ $MGL1^+$ $CD206^+$ $ST2^+$ $CD11c^-$ and represent the resident ATM population localized to interstitial spaces between adipocytes. These cells express many, but not all, markers of alternatively activated M2 macrophages. This redefinition leaves room to define new

ATM types as the examination of ATMs is broadened to include different fat depots and to define the properties of human ATMs.

MATERIALS AND METHODS

Animals and animal care. *Mgl1*$^{-/-}$ mice on a C57BL/6 background were provided by the Consortium for Functional Glycomics Core F. Male C57BL/6 mice were obtained from Jackson ImmunoResearch Laboratories. *Ccr2*$^{-/-}$ mice were provided by S. Kunkel (University of Michigan, Ann Arbor, MI). DIO was induced by feeding male mice a HFD consisting of 60% of calories from fat (Research Diets, Inc.) starting at 6–8 wk of age for 16–18 wk. Control mice were fed a ND consisting of 4.5% fat (5002; LabDiet). Animals were housed in a specific pathogen–free facility with a 12 h light/12 h dark cycle and given free access to food and water. All animal use was in compliance with the Institute of Laboratory Animal Research Guide for the Care and Use of Laboratory Animals and approved by the University Committee on Use and Care of Animals at the University of Michigan.

Reagents and antibodies. Anti-CD206/Mannose receptor, anti-CD301, and anti-7/4 Neutrophil were obtained from AbD Serotec. Anti-CD301/MGL1 and anti-ST2 antibodies were obtained from Abcam. Anti-F4/80, biotinylated anti-Lewis X (SSEA-1), and anti-Mac2 antibodies were obtained from eBioscience. Fc-block and anti-Ly6G antibodies were obtained from BD Biosciences. Isolectin-Alexa Fluor 647 was obtained from Invitrogen.

Microscopy. Immunofluorescence was performed as previously described (Lumeng et al., 2008). In brief, mice were perfused with 1% paraformaldehyde for fixation before dissecting fat pads. Samples were incubated en bloc in primary and secondary antibodies in 5% BSA in PBS. Imaging analysis was performed on an Olympus FluoView confocal microscope or an Olympus inverted microscope for epifluorescence. Image capture was performed with FluoView software or an Olympus DP72 charge-coupled device camera. Confocal images were pseudocolored in FluoView or ImageJ (National Institutes of Health). Composite images were generated using Adobe Photoshop. H&E-stained sections were imaged and adipocyte size was assessed by manually delineating adipocyte membranes and calculating cross-sectional area in ImageJ.

Flow cytometry. Analysis of adipose tissue stromal vascular fraction (SVF) by flow cytometry was performed as previously described (Lumeng et al., 2008). In brief, after collagenase digestion, adipose tissue cell suspensions were spun at 500 g for 5 min to separate floating adipocytes from the SVF pellet. After erythrocyte lysis, cells were incubated with Fc Block (BD) and stained according to manufacturer recommendation before analysis. TG elicited PMs were treated with 0.1 μg/ml LPS or vehicle for 6 h before collection. Cells were fixed, permeabilized (AbD Serotec), and stained with anti-TNF antibodies (BD) before analysis.

Gene expression analysis. Real-time quantitative RT-PCR was performed as previously described (Lumeng et al., 2007b, 2008).

Metabolic evaluation. Glucose tolerance tests were performed after IP injection with 0.7 g/kg dextrose. Insulin tolerance tests were performed after injection with 1 U/kg insulin. Glucose measurements were made with a glucometer (FreeStyle; Abbot Laboratories). Serum fasting insulin levels were determined by ELISA (Crystalchem Inc.). Oxygen consumption (VO2), carbon dioxide production, spontaneous motor activity, and food intake were measured using the Comprehensive Laboratory Monitoring System (CLAMS; Columbus Instruments) in the University of Michigan Animal Phenotyping Core. Body composition was determined using a Minispec NMR analyzer (Bruker Optics). FFA levels were assessed in duplicate using colorimetric assays (Zen-Bio Inc.).

Cell culture and adhesion assays. Thioglycollate-elicited PMs were isolated after i.p. injection of 3 ml of 3% Brewers TG by lavage with ice-cold PBS. Cells were enriched by adhesion to plastic and cultured in DMEM with 10% heat-inactivated fetal bovine serum (Invitrogen). 3T3-L1 adipocytes were grown and differentiated as previously described (Baumann et al., 2000). For in vitro adhesion assays, 0.5×10^6 CFSE-labeled monocytes from either genotype were added to differentiated adipocytes or confluent bEnd.3 monolayers in 12-well dishes for 30 min at 37°C. In some experiments, bEnd.3 cells were treated for 3 h with 50 ng/ml recombinant TNF (Sigma-Aldrich) before the addition of monocytes. After adhesion, wells were washed three times in PBS, and then fixed in 10% formalin. Adherent cells were quantitated after DAPI staining and imaging at 200× to enumerate monocytes in direct contact with adipocytes and normalized to the number of adipocytes per high power field.

Adoptive transfer of labeled monocytes. Monocytes were isolated from single-cell suspensions from spleen by Ficoll gradient (GE Healthcare). After washing, cells were labeled with by incubation with 5 μM CFSE in PBS and quenched with serum containing media. After washing in PBS, cells were counted and 2×10^6 cells were injected I.V. (retroorbital) in 200 μl total volume. 24 and 72 h after injection, blood was obtained by tail bleed in heparinized capillary tubes and stained for flow cytometry after erythrocyte lysis. CFSE$^+$ 7/4^{hi} CD11b$^+$ cells in the monocyte gate were quantitated and expressed as a percentage of all 7/4^{hi} CD11b$^+$ cells.

Statistical analysis. Statistical comparisons made using Student's *t* tests with significance defined as a P value <0.05. Graphs presented as mean and errors bars represent standard error of the mean.

This work was funded by National Institutes of Health grants DK078851 (C.N. Lumeng) and DK060591 (A.R. Saltiel) and the Ferrantino Investigator Award from the University of Michigan Dept. of Pediatrics and Communicable Diseases (C.N. Lumeng). This work utilized the Animal Phenotyping and Cell and Molecular Biology Cores of the Michigan Diabetes Research and Training Center funded by DK020572 from the National Institute of Diabetes and Digestive and Kidney Diseases. The *Mgl1* KO mice were provided by The Consortium for Functional Glycomics funded by NIGMS - GM62116.

The authors have no conflicting financial interests.

Submitted: 18 June 2009
Accepted: 11 November 2009

REFERENCES

Arkan, M.C., A.L. Hevener, F.R. Greten, S. Maeda, Z.W. Li, J.M. Long, A. Wynshaw-Boris, G. Poli, J. Olefsky, and M. Karin. 2005. IKK-beta links inflammation to obesity-induced insulin resistance. *Nat. Med.* 11:191–198. doi:10.1038/nm1185

Auffray, C., D. Fogg, M. Garfa, G. Elain, O. Join-Lambert, S. Kayal, S. Sarnacki, A. Cumano, G. Lauvau, and F. Geissmann. 2007. Monitoring of blood vessels and tissues by a population of monocytes with patrolling behavior. *Science.* 317:666–670. doi:10.1126/science.1142883

Baumann, C.A., V. Ribon, M. Kanzaki, D.C. Thurmond, S. Mora, S. Shigematsu, P.E. Bickel, J.E. Pessin, and A.R. Saltiel. 2000. CAP defines a second signalling pathway required for insulin-stimulated glucose transport. *Nature.* 407:202–207. doi:10.1038/35025089

Bouhlel, M.A., B. Derudas, E. Rigamonti, R. Dièvart, J. Brozek, S. Haulon, C. Zawadzki, B. Jude, G. Torpier, N. Marx, et al. 2007. PPARgamma activation primes human monocytes into alternative M2 macrophages with anti-inflammatory properties. *Cell Metab.* 6:137–143. doi:10.1016/j.cmet.2007.06.010

Bourlier, V., A. Zakaroff-Girard, A. Miranville, S. De Barros, M. Maumus, C. Sengenes, J. Galitzky, M. Lafontan, F. Karpe, K.N. Frayn, and A. Bouloumié. 2008. Remodeling phenotype of human subcutaneous adipose tissue macrophages. *Circulation.* 117:806–815. doi:10.1161/CIRCULATIONAHA.107.724096

Brint, E.K., D. Xu, H. Liu, A. Dunne, A.N. McKenzie, L.A. O'Neill, and F.Y. Liew. 2004. ST2 is an inhibitor of interleukin 1 receptor and Toll-like receptor 4 signaling and maintains endotoxin tolerance. *Nat. Immunol.* 5:373–379. doi:10.1038/ni1050

Charo, I.F. 2007. Macrophage polarization and insulin resistance: PPARgamma in control. *Cell Metab.* 6:96–98. doi:10.1016/j.cmet.2007.07.006

Cinti, S., G. Mitchell, G. Barbatelli, I. Murano, E. Ceresi, E. Faloia, S. Wang, M. Fortier, A.S. Greenberg, and M.S. Obin. 2005. Adipocyte death defines macrophage localization and function in adipose tissue of obese mice and humans. *J. Lipid Res.* 46:2347–2355. doi:10.1194/jlr.M500294-JLR200

Coenen, K.R., M.L. Gruen, R.S. Lee-Young, M.J. Puglisi, D.H. Wasserman, and A.H. Hasty. 2009. Impact of macrophage toll-like receptor 4 deficiency on macrophage infiltration into adipose tissue and the artery wall in mice. *Diabetologia.* 52:318–328. doi:10.1007/s00125-008-1221-7

Coppack, S.W. 2001. Pro-inflammatory cytokines and adipose tissue. *Proc. Nutr. Soc.* 60:349–356. doi:10.1079/PNS2001110

Degasperi, G.R., R.G. Denis, J. Morari, C. Solon, B. Geloneze, C. Stabe, J.C. Pareja, A.E. Vercesi, and L.A. Velloso. 2009. Reactive oxygen species production is increased in the peripheral blood monocytes of obese patients. *Metabolism.* 58:1087–1095.

Dupasquier, M., P. Stoitzner, H. Wan, D. Cerqueira, A. van Oudenaren, J.S. Voerman, K. Denda-Nagai, T. Irimura, G. Raes, N. Romani, and P.J. Leenen. 2006. The dermal microenvironment induces the expression of the alternative activation marker CD301/mMGL in mononuclear phagocytes, independent of IL-4/IL-13 signaling. *J. Leukoc. Biol.* 80:838–849. doi:10.1189/jlb.1005564

Feuerer, M., L. Herrero, D. Cipolletta, A. Naaz, J. Wong, A. Nayer, J. Lee, A.B. Goldfine, C. Benoist, S. Shoelson, and D. Mathis. 2009. Lean, but not obese, fat is enriched for a unique population of regulatory T cells that affect metabolic parameters. *Nat. Med.* 15:930–939. doi:10.1038/nm.2002

Geissmann, F., S. Jung, and D.R. Littman. 2003. Blood monocytes consist of two principal subsets with distinct migratory properties. *Immunity.* 19:71–82. doi:10.1016/S1074-7613(03)00174-2

Ghanim, H., A. Aljada, D. Hofmeyer, T. Syed, P. Mohanty, and P. Dandona. 2004. Circulating mononuclear cells in the obese are in a proinflammatory state. *Circulation.* 110:1564–1571. doi:10.1161/01.CIR.0000142055.53122.FA

Gordon, S. 2007. Macrophage heterogeneity and tissue lipids. *J. Clin. Invest.* 117:89–93. doi:10.1172/JCI30992

Gordon, S., and P.R. Taylor. 2005. Monocyte and macrophage heterogeneity. *Nat. Rev. Immunol.* 5:953–964. doi:10.1038/nri1733

Hevener, A.L., J.M. Olefsky, D. Reichart, M.T. Nguyen, G. Bandyopadyhay, H.Y. Leung, M.J. Watt, C. Benner, M.A. Febbraio, A.K. Nguyen, et al. 2007. Macrophage PPAR gamma is required for normal skeletal muscle and hepatic insulin sensitivity and full antidiabetic effects of thiazolidinediones. *J. Clin. Invest.* 117:1658–1669. doi:10.1172/JCI31561

Hotamisligil, G.S. 2006. Inflammation and metabolic disorders. *Nature.* 444:860–867. doi:10.1038/nature05485

Hotamisligil, G.S., P. Arner, J.F. Caro, R.L. Atkinson, and B.M. Spiegelman. 1995. Increased adipose tissue expression of tumor necrosis factor-alpha in human obesity and insulin resistance. *J. Clin. Invest.* 95:2409–2415. doi:10.1172/JCI117936

Inouye, K.E., H. Shi, J.K. Howard, C.H. Daly, G.M. Lord, B.J. Rollins, and J.S. Flier. 2007. Absence of CC chemokine ligand 2 does not limit obesity-associated infiltration of macrophages into adipose tissue. *Diabetes.* 56:2242–2250. doi:10.2337/db07-0425

Kanda, H., S. Tateya, Y. Tamori, K. Kotani, K. Hiasa, R. Kitazawa, S. Kitazawa, H. Miyachi, S. Maeda, K. Egashira, and M. Kasuga. 2006. MCP-1 contributes to macrophage infiltration into adipose tissue, insulin resistance, and hepatic steatosis in obesity. *J. Clin. Invest.* 116:1494–1505. doi:10.1172/JCI26498

Kang, K., S.M. Reilly, V. Karabacak, M.R. Gangl, K. Fitzgerald, B. Hatano, and C.H. Lee. 2008. Adipocyte-derived Th2 cytokines and myeloid PPARdelta regulate macrophage polarization and insulin sensitivity. *Cell Metab.* 7:485–495. doi:10.1016/j.cmet.2008.04.002

Kim, J.Y., E. van de Wall, M. Laplante, A. Azzara, M.E. Trujillo, S.M. Hofmann, T. Schraw, J.L. Durand, H. Li, G. Li, et al. 2007. Obesity-associated improvements in metabolic profile through expansion of adipose tissue. *J. Clin. Invest.* 117:2621–2637. doi:10.1172/JCI31021

Kirk, E.A., Z.K. Sagawa, T.O. McDonald, K.D. O'Brien, and J.W. Heinecke. 2008. MCP-1 deficiency fails to restrain macrophage infiltration into adipose tissue. *Diabetes.* 57:1254–1261. doi:10.2337/db07-1061

Kumamoto, Y., N. Higashi, K. Denda-Nagai, M. Tsuiji, K. Sato, P.R. Crocker, and T. Irimura. 2004. Identification of sialoadhesin as a dominant lymph node counter-receptor for mouse macrophage galactose-type C-type lectin 1. *J. Biol. Chem.* 279:49274–49280. doi:10.1074/jbc.M409300200

Landsman, L., L. Bar-On, A. Zernecke, K.W. Kim, R. Krauthgamer, E. Shagdarsuren, S.A. Lira, I.L. Weissman, C. Weber, and S. Jung. 2009. CX3CR1 is required for monocyte homeostasis and atherogenesis by promoting cell survival. *Blood.* 113:963–972. doi:10.1182/blood-2008-07-170787

Lowe, J.B. 2003. Glycan-dependent leukocyte adhesion and recruitment in inflammation. *Curr. Opin. Cell Biol.* 15:531–538. doi:10.1016/j.ceb.2003.08.002

Lumeng, C.N., S.M. Deyoung, and A.R. Saltiel. 2007a. Macrophages block insulin action in adipocytes by altering expression of signaling and glucose transport proteins. *Am. J. Physiol. Endocrinol. Metab.* 292:E166–E174. doi:10.1152/ajpendo.00284.2006

Lumeng, C.N., J.L. Bodzin, and A.R. Saltiel. 2007b. Obesity induces a phenotypic switch in adipose tissue macrophage polarization. *J. Clin. Invest.* 117:175–184. doi:10.1172/JCI29881

Lumeng, C.N., J.B. DelProposto, D.J. Westcott, and A.R. Saltiel. 2008. Phenotypic switching of adipose tissue macrophages with obesity is generated by spatiotemporal differences in macrophage subtypes. *Diabetes.* 57:3239–3246. doi:10.2337/db08-0872

Martinez, M., M. Joffraud, S. Giraud, B. Baïsse, M.P. Bernimoulin, M. Schapira, and O. Spertini. 2005. Regulation of PSGL-1 interactions with L-selectin, P-selectin, and E-selectin: role of human fucosyltransferase-IV and -VII. *J. Biol. Chem.* 280:5378–5390. doi:10.1074/jbc.M410899200

Murano, I., G. Barbatelli, V. Parisani, C. Latini, G. Muzzonigro, M. Castellucci, and S. Cinti. 2008. Dead adipocytes, detected as crown-like structures, are prevalent in visceral fat depots of genetically obese mice. *J. Lipid Res.* 49:1562–1568. doi:10.1194/jlr.M800019-JLR200

Neels, J.G., and J.M. Olefsky. 2006. Inflamed fat: what starts the fire? *J. Clin. Invest.* 116:33–35. doi:10.1172/JCI27280

Nguyen, M.T., S. Favelyukis, A.K. Nguyen, D. Reichart, P.A. Scott, A. Jenn, R. Liu-Bryan, C.K. Glass, J.G. Neels, and J.M. Olefsky. 2007. A subpopulation of macrophages infiltrates hypertrophic adipose tissue and is activated by free fatty acids via Toll-like receptors 2 and 4 and JNK-dependent pathways. *J. Biol. Chem.* 282:35279–35292. doi:10.1074/jbc.M706762200

Nishimura, S., I. Manabe, M. Nagasaki, K. Seo, H. Yamashita, Y. Hosoya, M. Ohsugi, K. Tobe, T. Kadowaki, R. Nagai, and S. Sugiura. 2008. In vivo imaging in mice reveals local cell dynamics and inflammation in obese adipose tissue. *J. Clin. Invest.* 118:710–721.

Odegaard, J.I., R.R. Ricardo-Gonzalez, M.H. Goforth, C.R. Morel, V. Subramanian, L. Mukundan, A. Red Eagle, D. Vats, F. Brombacher, A.W. Ferrante, and A. Chawla. 2007. Macrophage-specific PPARgamma controls alternative activation and improves insulin resistance. *Nature.* 447:1116–1120. doi:10.1038/nature05894

Poland, D.C., C.G. Schalkwijk, C.D. Stehouwer, C.A. Koeleman, B. van het Hof, and W. van Dijk. 2001. Increased alpha3-fucosylation of alpha1-acid glycoprotein in Type I diabetic patients is related to vascular function. *Glycoconj. J.* 18:261–268. doi:10.1023/A:1012412908983

Saba, K., K. Denda-Nagai, and T. Irimura. 2009. A C-type lectin MGL1/CD301a plays an anti-inflammatory role in murine experimental colitis. *Am. J. Pathol.* 174:144–152. doi:10.2353/ajpath.2009.080235

Sartipy, P., and D.J. Loskutoff. 2003. Monocyte chemoattractant protein 1 in obesity and insulin resistance. *Proc. Natl. Acad. Sci. USA.* 100:7265–7270. doi:10.1073/pnas.1133870100

Serbina, N.V., and E.G. Pamer. 2006. Monocyte emigration from bone marrow during bacterial infection requires signals mediated by chemokine receptor CCR2. *Nat. Immunol.* 7:311–317. doi:10.1038/ni1309

Shi, H., M.V. Kokoeva, K. Inouye, I. Tzameli, H. Yin, and J.S. Flier. 2006. TLR4 links innate immunity and fatty acid-induced insulin resistance. *J. Clin. Invest.* 116:3015–3025. doi:10.1172/JCI28898

Singh, S.K., I. Streng-Ouwehand, M. Litjens, D.R. Weelij, J.J. García-Vallejo, S.J. van Vliet, E. Saeland, and Y. van Kooyk. 2009. Characterization of murine MGL1 and MGL2 C-type lectins: distinct glycan specificities and tumor binding properties. *Mol. Immunol.* 46:1240–1249. doi:10.1016/j.molimm.2008.11.021

Solinas, G., C. Vilcu, J.G. Neels, G.K. Bandyopadhyay, J.L. Luo, W. Naugler, S. Grivennikov, A. Wynshaw-Boris, M. Scadeng, J.M. Olefsky, and M. Karin. 2007. JNK1 in hematopoietically derived cells contributes to diet-induced inflammation and insulin resistance without affecting obesity. *Cell Metab.* 6:386–397. doi:10.1016/j.cmet.2007.09.011

Takahashi, K., S. Mizuarai, H. Araki, S. Mashiko, A. Ishihara, A. Kanatani, H. Itadani, and H. Kotani. 2003. Adiposity elevates plasma MCP-1 levels leading to the increased CD11b-positive monocytes in mice. *J. Biol. Chem.* 278:46654–46660. doi:10.1074/jbc.M309895200

Tsou, C.L., W. Peters, Y. Si, S. Slaymaker, A.M. Aslanian, S.P. Weisberg, M. Mack, and I.F. Charo. 2007. Critical roles for CCR2 and MCP-3 in monocyte mobilization from bone marrow and recruitment to inflammatory sites. *J. Clin. Invest.* 117:902–909. doi:10.1172/JCI29919

Tsuiji, M., M. Fujimori, Y. Ohashi, N. Higashi, T.M. Onami, S.M. Hedrick, and T. Irimura. 2002. Molecular cloning and characterization of a novel mouse macrophage C-type lectin, mMGL2, which has a distinct carbohydrate specificity from mMGL1. *J. Biol. Chem.* 277:28892–28901. doi:10.1074/jbc.M203774200

van Kooyk, Y. 2008. C-type lectins on dendritic cells: key modulators for the induction of immune responses. *Biochem. Soc. Trans.* 36:1478–1481. doi:10.1042/BST0361478

van Vliet, S.J., S.I. Gringhuis, T.B. Geijtenbeek, and Y. van Kooyk. 2006. Regulation of effector T cells by antigen-presenting cells via interaction of the C-type lectin MGL with CD45. *Nat. Immunol.* 7:1200–1208. doi:10.1038/ni1390

van Vliet, S.J., E. Saeland, and Y. van Kooyk. 2008a. Sweet preferences of MGL: carbohydrate specificity and function. *Trends Immunol.* 29:83–90. doi:10.1016/j.it.2007.10.010

van Vliet, S.J., L.C. Paessens, V.C. Broks-van den Berg, T.B. Geijtenbeek, and Y. van Kooyk. 2008b. The C-type lectin macrophage galactose-type lectin impedes migration of immature APCs. *J. Immunol.* 181:3148–3155.

Weisberg, S.P., D. McCann, M. Desai, M. Rosenbaum, R.L. Leibel, and A.W. Ferrante Jr. 2003. Obesity is associated with macrophage accumulation in adipose tissue. *J. Clin. Invest.* 112:1796–1808.

Weisberg, S.P., D. Hunter, R. Huber, J. Lemieux, S. Slaymaker, K. Vaddi, I. Charo, R.L. Leibel, and A.W. Ferrante Jr. 2006. CCR2 modulates inflammatory and metabolic effects of high-fat feeding. *J. Clin. Invest.* 116:115–124. doi:10.1172/JCI24335

Xu, H., G.T. Barnes, Q. Yang, G. Tan, D. Yang, C.J. Chou, J. Sole, A. Nichols, J.S. Ross, L.A. Tartaglia, and H. Chen. 2003. Chronic inflammation in fat plays a crucial role in the development of obesity-related insulin resistance. *J. Clin. Invest.* 112:1821–1830.

Yuita, H., M. Tsuiji, Y. Tajika, Y. Matsumoto, K. Hirano, N. Suzuki, and T. Irimura. 2005. Retardation of removal of radiation-induced apoptotic cells in developing neural tubes in macrophage galactose-type C-type lectin-1-deficient mouse embryos. *Glycobiology.* 15:1368–1375. doi:10.1093/glycob/cwj028

Zeyda, M., D. Farmer, J. Todoric, O. Aszmann, M. Speiser, G. Györi, G.J. Zlabinger, and T.M. Stulnig. 2007. Human adipose tissue macrophages are of an anti-inflammatory phenotype but capable of excessive pro-inflammatory mediator production. *Int J Obes (Lond).* 31:1420–1428. doi:10.1038/sj.ijo.0803632